D* production in Deep Inelastic Scattering at Hera and $F_2^{c\bar{c}}$

J.Roldán
DESY

on behalf of the ZEUS Collaboration

Introduction

ZEUS 94 results

ZEUS 95 preliminary results on $F_2^{c\bar{c}}$

Summary

Kinematics of Charm production

$$Q^2 \equiv -(p_e - p'_e)^2$$
$$W^2 \equiv (p_P + p_\gamma)^2 \qquad \gamma^* \text{ p CM energy}$$

1-body kinematics processes : charm from sea or IC (flavour excitation)

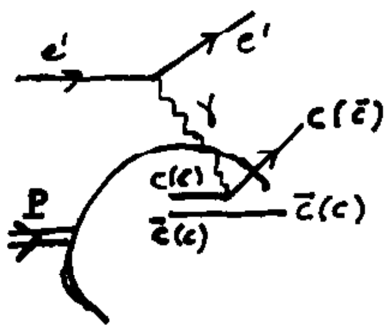

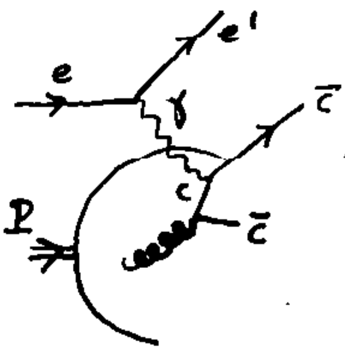

for $Q^2 > \mu_c^2$ $(= 4m_c^2)$

- p_T of charms unbalanced in γ^* p frame (recoils against P remnant)
- charm present in initial state (parton) and final state
- IC (à la Brodsky)
- in PQCD $g \to c\bar{c}$ ($Q^2 > \mu_c^2$)), one charm is expectator

2-body kinematics processes : PGF pQCD

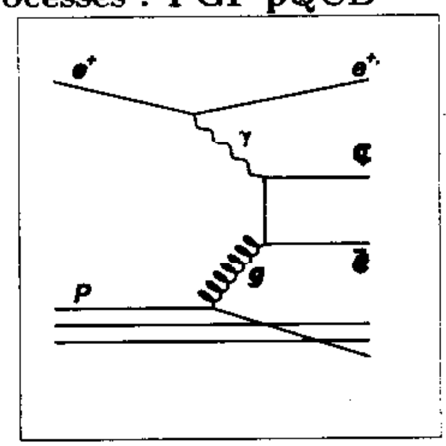

- c and $\bar{c}$ back to back in γ^* p frame
- charm appears only in final state
- $W^2 = Q^2(1-x)/x > 4m_c^2 \to$ allowed for $Q^2 < 4m_c^2$ at low x

Charm production in pQCD : approaches to global data analises

1) Old approach : Massless Parton Evolution ($m_c = 0$)

- $c(x, Q^2) = 0$ for $Q^2 < \mu_c^2$ ($\sim 4m_c^2$)
- $n_f = 3 + \Theta(Q^2 - \mu_c^2)$
- massless evol. for $Q^2 > \mu_c^2$, OK for asymptotic region $Q^2 >> \mu_c^2$
- $c(x, Q^2)$ arbitrary function fitted to data
- old MRS,CTEQ parametrisations

2) Fixed Flavour Number (FFN) scheme ($m_c \neq 0$)

- $c(x, Q^2) = 0$ for all Q^2 and $n_f = 3$ (no charm as parton)
- problems in asymptotic region due to large $log(Q^2/m_c)$
- All charm production due to PGF (calculated at any order in FOPT)
- right for threshold region $Q^2 \sim \mu_c^2$
- GRV94,CTEQ4F3, ZEUS and H1 NLO fits to F_2 data

3) VFN scheme (Aivazis et al.) or equivalent (MRRS) ($m_c \neq 0$)

- $c(x, Q^2)$ is calculable and predicted from pQCD from gluon and light quark densities
- Part of PGF is generated dynamically by pQCD $\rightarrow$ subtraction needed
- right limits for threshold (PGF) and asymptotic regions (Q^2 parton evolution)
- CTEQ4HQ, MRRS

DIS Event Selection

- **DIS event candidates are triggered by requiring a minimum of energy deposition in the electromganetic sections of the ZEUS Calorimeter (CAL) .**
- **e^+ identification is based on a neural network using CAL information.**
- **The efficiency of e^+ identification vary from 50 % for $E'_e = 8$ GeV to more than 90 % for $E'_e > 15 GeV$**

The following cuts are applied :

- $E'_e > 8\,GeV$
  (good e^+ id. eff.)
- $\delta \equiv \sum_i (E_i - p_{z_i}) > 35\,GeV$
  (removes photoproduction background and events with hard initial state radiation)

To reconstruct the kinematic variables y and Q^2 we use the Double Angle (DA) method.

The DIS kinematic region for the analysis is :

- **($5 < Q^2 < 100$) GeV^2**
- **$y < 0.7$ (consequence of $E'_e > 8\,GeV$)**

D* Identification

D* production is investigated in the decay channel

$$D^{*+} \rightarrow D^0\pi_S^+ \rightarrow (K^-\pi^+)\pi^+ + \text{c.c.}$$

$D^{*+} \rightarrow D^0\pi^+$ decays have a clear signature as a prominent peak at the end of the

$$\Delta M \equiv M(K\pi\pi_S) - M(K\pi)$$

spectrum.

- **Tracks from charged particles are reconstructed using the ZEUS Central Tracking Detector (CTD). It has a vertex resolution of 0.4 cm in the Z-direction and 0.1 cm in the XY plane.**

For the analysis the following requirements are made for the tracks :

- **Tracks must be associated to the** primary vertex **and must have more than** 20 hits/track **(The CTD spatial resolution does not allow the D^0 vertex to be distinguish from the primary vertex).**
- $p_T > 0.125$ GeV
- $|\eta| < 1.75$ ($\equiv 20^o < \theta < 160^o$)

Due the above requirements, D* production search is restricted to the following kinematic region :

- $p_T(D^*) > 1.3$ GeV (and also $p_T(D^*) < 9$ GeV)
- $|\eta(D^*)| < 1.5$

The procedure to find a D* is as follows :

1. **Combine pairs of oppositely charged tracks assumed in turn to be from a kaon or a pion and calculate the invariant mass $M(K\pi)$.**
2. **If** $(1.80 < M(K\pi) < 1.92)$ GeV, **combine this pair with a third track, assumed to be from a pion (π_S), and calculate $\Delta M = M(K\pi\pi_S) - M(K\pi)$.**

To reduce combinatorial background the additional cut

- $p_T(K,\pi) > 0.4$ GeV

has been applied.

The background under the signal can be estimated using the Wrong Charge (WC) combinations method :

- **counting the number of combinations which use pairs of tracks with the same charge when calculating $M(K\pi)$ and give a ΔM value in the signal region conveniently normalized to the region far away from the signal.**

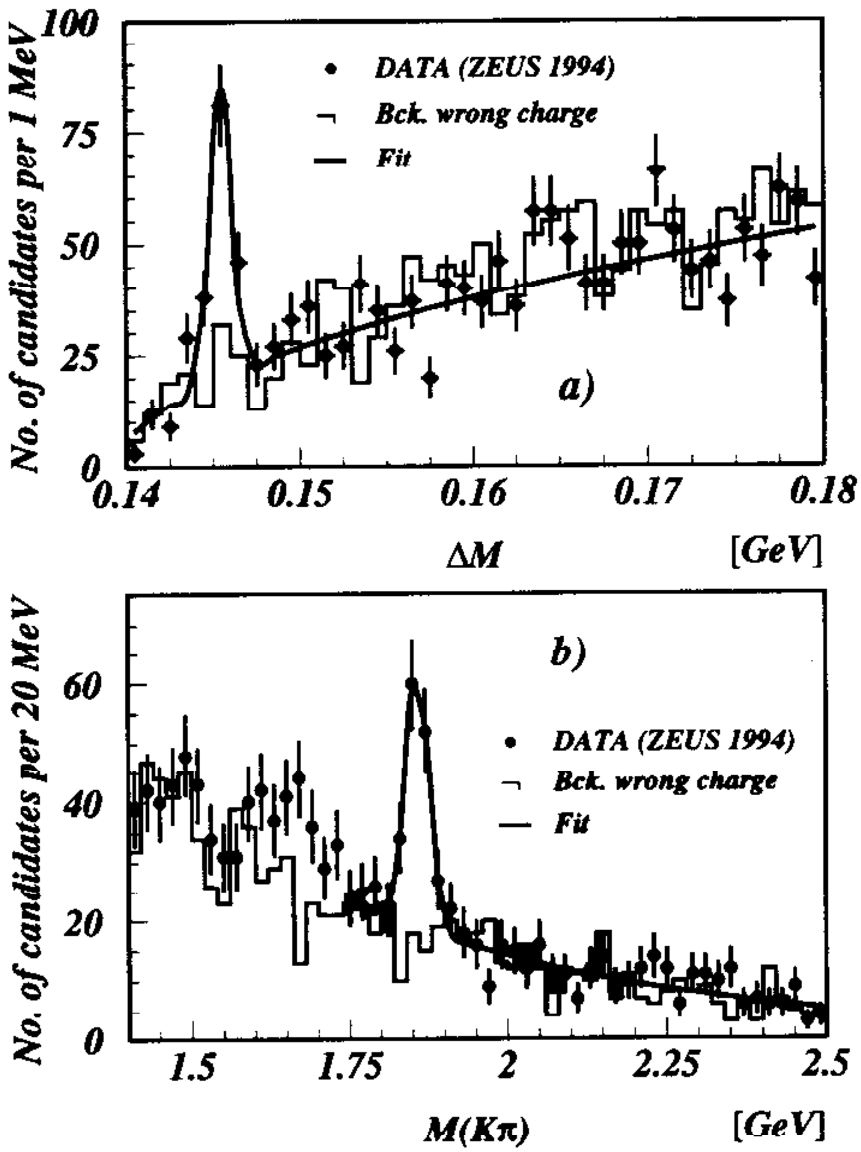

Up : ΔM distribution for $K\pi$ combinations in the region ($1.80 < M(K\pi) < 1.92$) GeV.
Down : $M(K\pi)$ invariant mass for the $K\pi\pi_s$ combinations in the signal region ($143 < \Delta M < 148$ MeV). No $M(D^0)$ window cut.

The solid histograms shows the $M(K\pi)$ and ΔM distributions for the wrong charge $K\pi$ combinations. The solid lines in both figures show the result from the fits.

A maximum likelihood fit to ΔM using a gaussian plus a background of the form $a(\Delta M - m_\pi)^b$ yields :

$$M(\mathrm{D}^*) - M(\mathrm{D}^0) = (145.44 \pm 0.01)\ \mathrm{MeV}$$

with a width of (0.65 ± 0.10) MeV.

The signal region is defined to be 143 $< \Delta M <$ 148 MeV, which corresponds to take $\sim 3\sigma$'s from the mean value of the fit.

The number of D* in the signal region after background subtraction is 122 ± 17 over a background of 95 ± 8.

The $M(K\pi)$ distribution is fitted using a gaussian plus an exponential background and gives

$$M(\mathrm{D}^0) = (1858 \pm 3)\ \mathrm{MeV}$$

The width of the signal is 19 ± 3 MeV, $\rightarrow$ the range (1.80,1.92) cooresponds to $\sim 3\sigma$'s deviation.

Detector Acceptance

Detector and trigger acceptance are determined using a GEANT based MC and different MC events generators :

DIS Selection Efficiency

- HERACLES + LEPTO (MEPS) + GRV-HO
- HERACLES + ARIADNE (CDMBGF) + MRSD-'

The average event selection efficiency is ~ 75 % (higher for large Q^2 and large y)

D* reconstruction efficiency

- AROMA : **LO PGF + PS + JETSET**
- HERWIG : **LO PGF + PS + Cluster Fragmentation**

The average D* reconstruction efficiency for the decay channel considered is ~ 38 %.

- **The total acceptance** *Acc* **is obtained convoluting the D* reconstruction efficiency with the DIS event selection efficiency.**

In overall, it is found to be ~ 30 %.

$D^{*\pm}$ cross sections in the restricted kinematic region

Cross sections are determined by :

$$\sigma(e^+p \to e^+ \mathrm{D}^* X) = \frac{\#\mathrm{D}^*}{(\mathcal{L} \cdot Acc)} \cdot \frac{1}{B(\mathrm{D}^{*+} \to \mathrm{D}^0\pi^+\,) \cdot B(\mathrm{D}^0 \to K^-\pi^+)}$$

where

$$\mathcal{L} = 2.95\, pb^{-1}$$

and

$$B(\mathrm{D}^{*+} \to \mathrm{D}^0\pi^+\,) \cdot B(\mathrm{D}^0 \to K^-\pi^+) = 0.0262 \pm 0.0010 \text{ (PDG value)}$$

The same procedure was followed dividing the signal in bins of W, Q^2, $\eta(D^*)$ and $p_T(D^*)$ to obtain the differential cross sections :

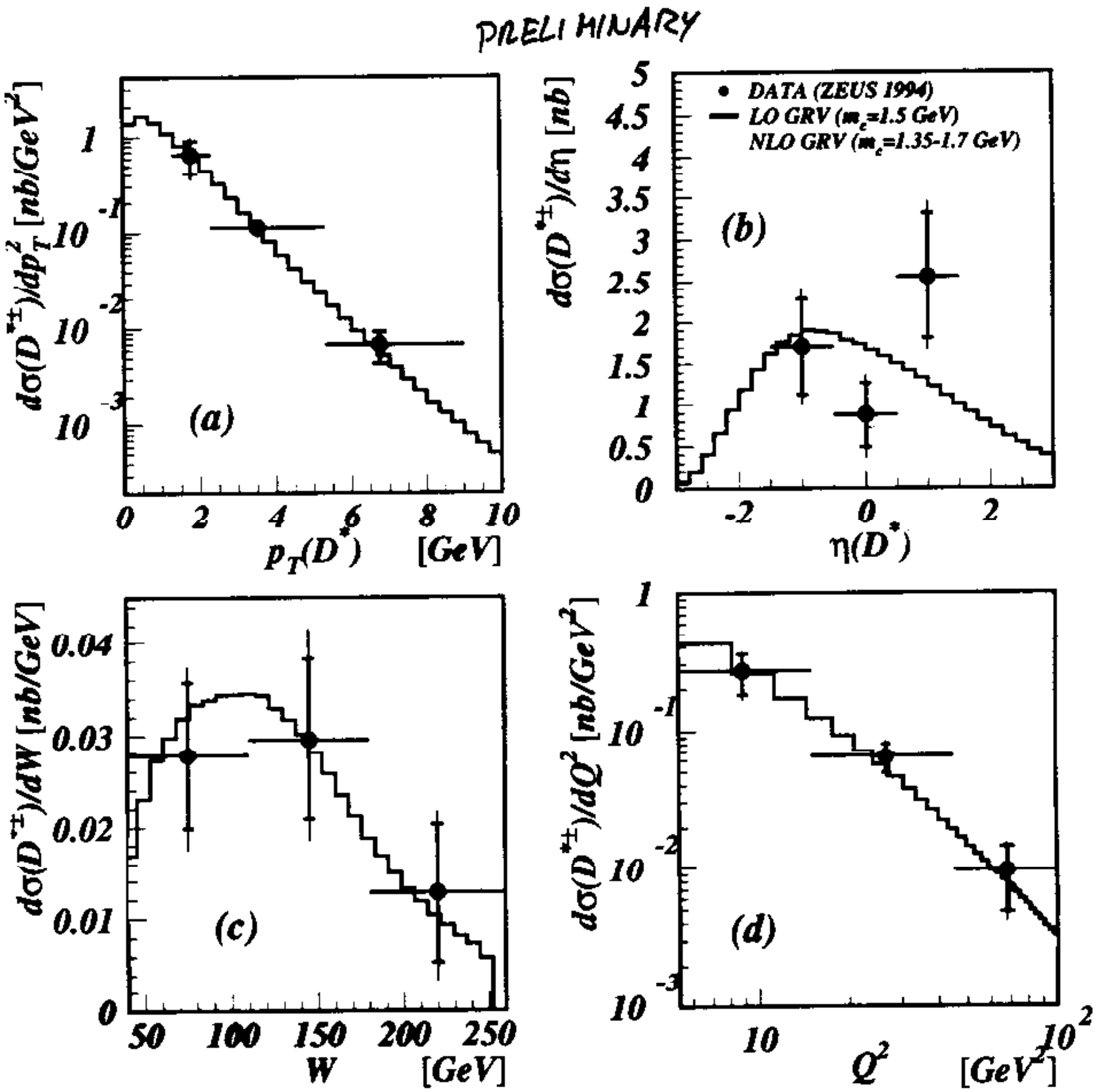

Differential cross sections for D* production versus $p_T(D^*)$, $\eta(D^*)$, W and Q^2. The inner error bars show the statistical errors and the outer ones correspond to the statistic and systematic errors added in quadrature. The NLO PGF prediction of Smith et al. calculated with the NLO gluon densities of GRV94 is shown as a band (varying m_c from 1.35 to 1.7). The LO calculation (with the LO GRV94 gluon desity) is shown as histograms.

D* fractional momentum distribution in the $\gamma^* p$ system

$$x_{D^*} = \frac{2|\vec{p}^{\,*}_{D^*}|}{W}$$

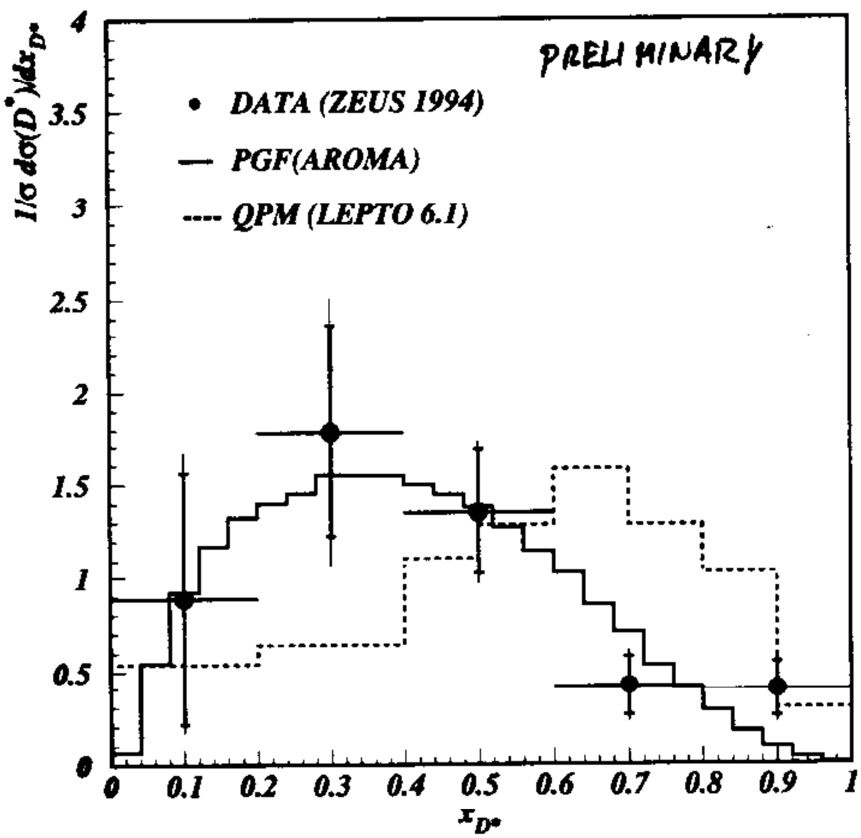

The distribution is expected to be centered at $x_{D^*} < 0.5$ for PGF and peaked at high x_{D^*} values for charm production from the proton sea. Both MC in the plot use the proton density of MRSD$-'$. The shape of our data distribution is compatible with PGF, in accord with the H1 result.

Charm $c\bar{c}$ cross sections

Measured $D^{*\pm}$ cross sections are extrapolated to the full $\{p_T(D^*), \eta(D^*)\}$ range using NLO analitic calculations from Smith et al.

Then $\sigma_{c\bar{c}}$ is obtained according to

$$\sigma(e^+p \to e^+\, c\bar{c}\, X) = \frac{1}{2} \cdot \frac{\sigma(e^+p \to e^+\, D^*\, X)}{P(c \to D^*)}.$$

using $P(c \to D^*) = 0.26 \pm 0.02$ (OPAL result).

By dividing the data in two Q^2 bins (5,10) and (10,100) we obtain :

$$\sigma\,(e^+p \;\to\; e^+\, c\bar{c}\, X) =$$

- $13.5 \pm 5.2 \pm 1.8\,^{+1.6}_{-1.2}$ nb for $5 < Q^2 < 10\,\mathrm{GeV}^2$
- $12.5 \pm 3.1 \pm 1.8\,^{+1.5}_{-1.1}$ nb for $10 < Q^2 < 100\,\mathrm{GeV}^2$

(The value for the $10 < Q^2 < 100$ GeV^2 is compatible with the H1 result : $15.1 \pm 1.8\,^{+2.4}_{-2.0} \pm 1.2$nb)

	$\sigma_{p_T,\eta}$ [nb]	σ_1 [nb]	σ_2 [nb]
Data	**$5.3 \pm 1.0 \pm 0.8$**	**$13.5 \pm 5.2 \pm 1.8^{+1.6}_{-1.2}$**	**$12.5 \pm 3.1 \pm 1.8^{+1.5}_{-1.1}$**
AROMA	4.57	12.6	14.2
PGF LO	4.79	11.0	12.4
PGF NLO	4.15	9.4	11.1

$F_2^{c\bar{c}}(x, Q^2)$ results

We divide the data in four Q^2 regions, each of them divided in two y regions :

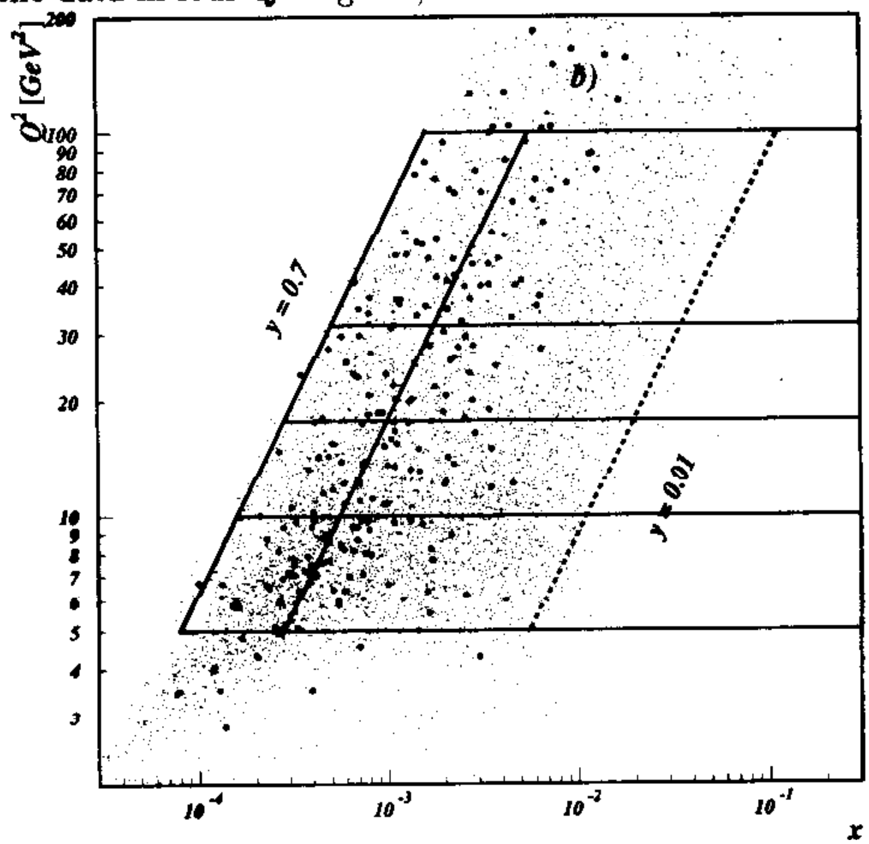

and give $F_2^{c\bar{c}}(x, Q^2)$ according to

$$\frac{d^2\sigma^{c\bar{c}}}{dx dQ^2} = \frac{2\pi\alpha^2}{Q^4 x}[(1 + (1 - y)^2) F_2^{c\bar{c}}(x, Q^2)]$$

where the F_3 contribution to the cross section (from Z^o) is neglegted and the $F_L^{c\bar{c}}$ has been estimated to be < 2 % and no correction has been made for its effect.

PRELIMINARY

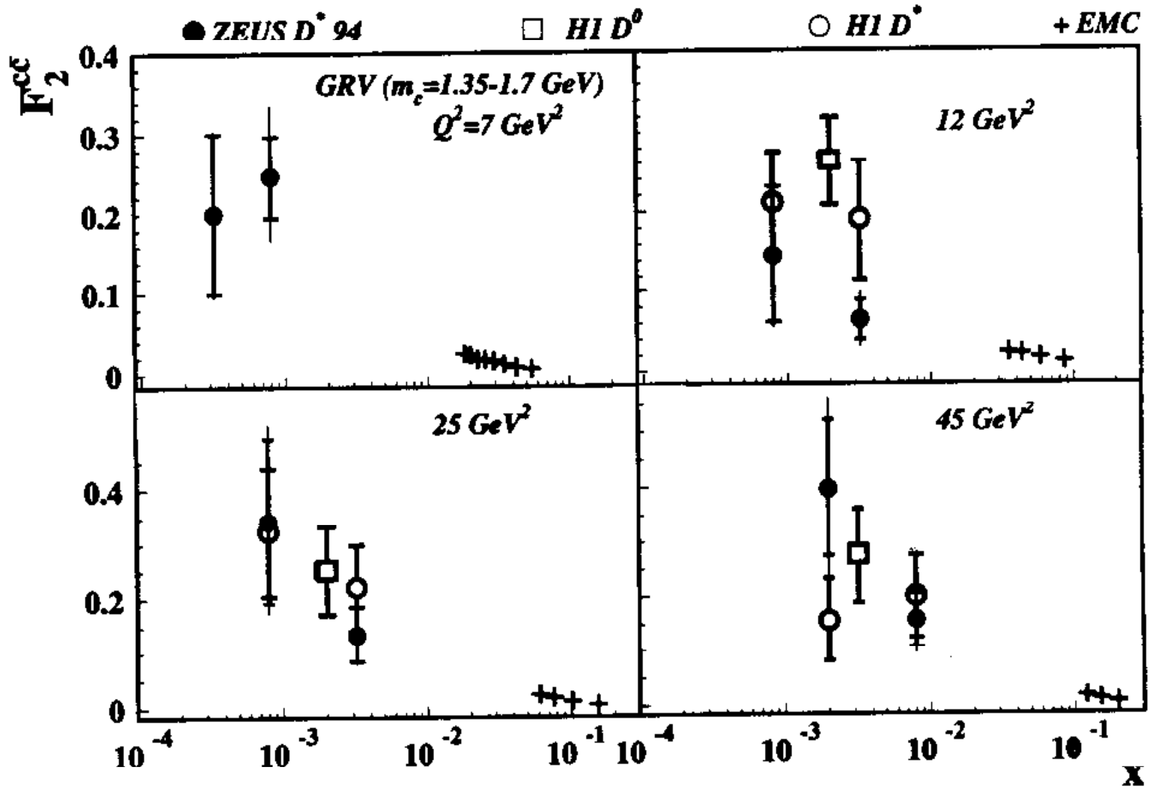

- Compared to the EMC measurements (large x) $F_2^{c\bar{c}}$ is found to rise as x decreases. The rise is described by NLO QCD calculations when using a gluon density consistent with that extracted from the scaling violations in the proton structure function F_2 measured at HERA $\rightarrow$ independent check for gluon density
- the ratio $F_2^{c\bar{c}}/F_2$ is about 25% compared to $\mathcal{O}(10^{-2})$ at high x.
- The use of CTEQ4F3 and MRRS gluon distributions give same result within 5 % [redacted].(?)

ZEUS 95 DATA

($1 < Q^2 < 600$) GeV^2

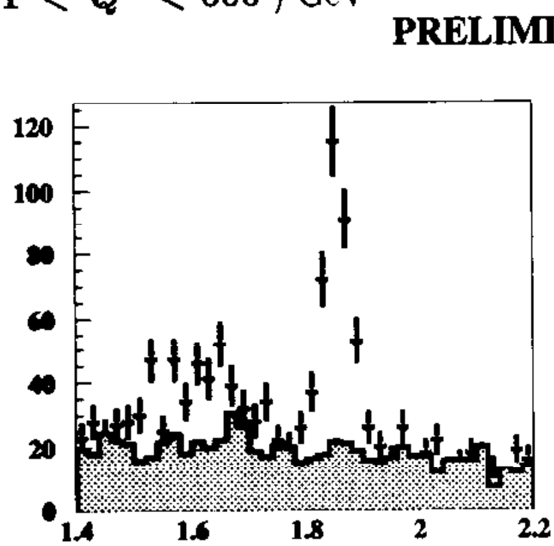

Luminosity 6.36 pb^{-1}

PRELIMINARY ZEUS 95

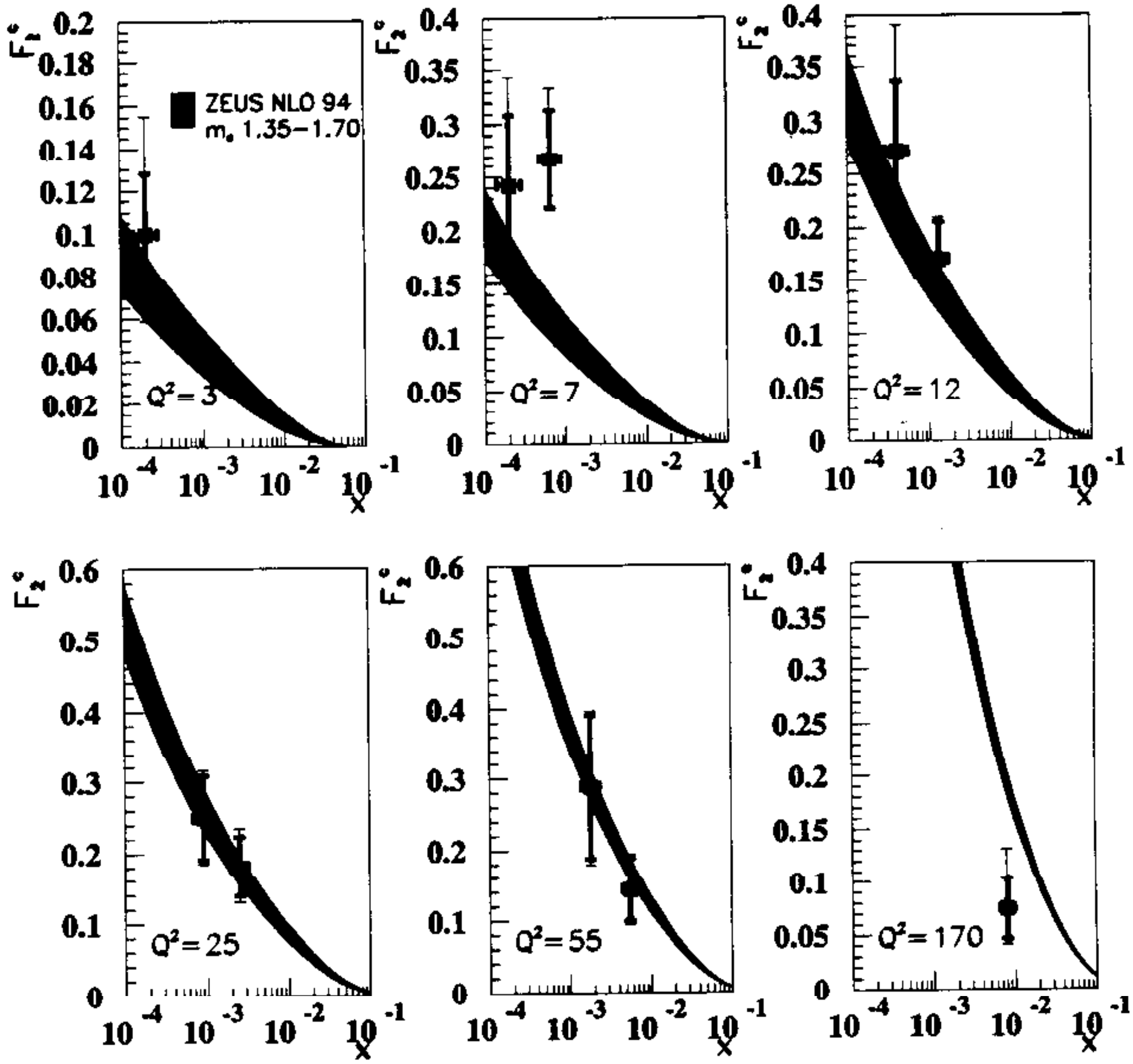

ZEUS 94

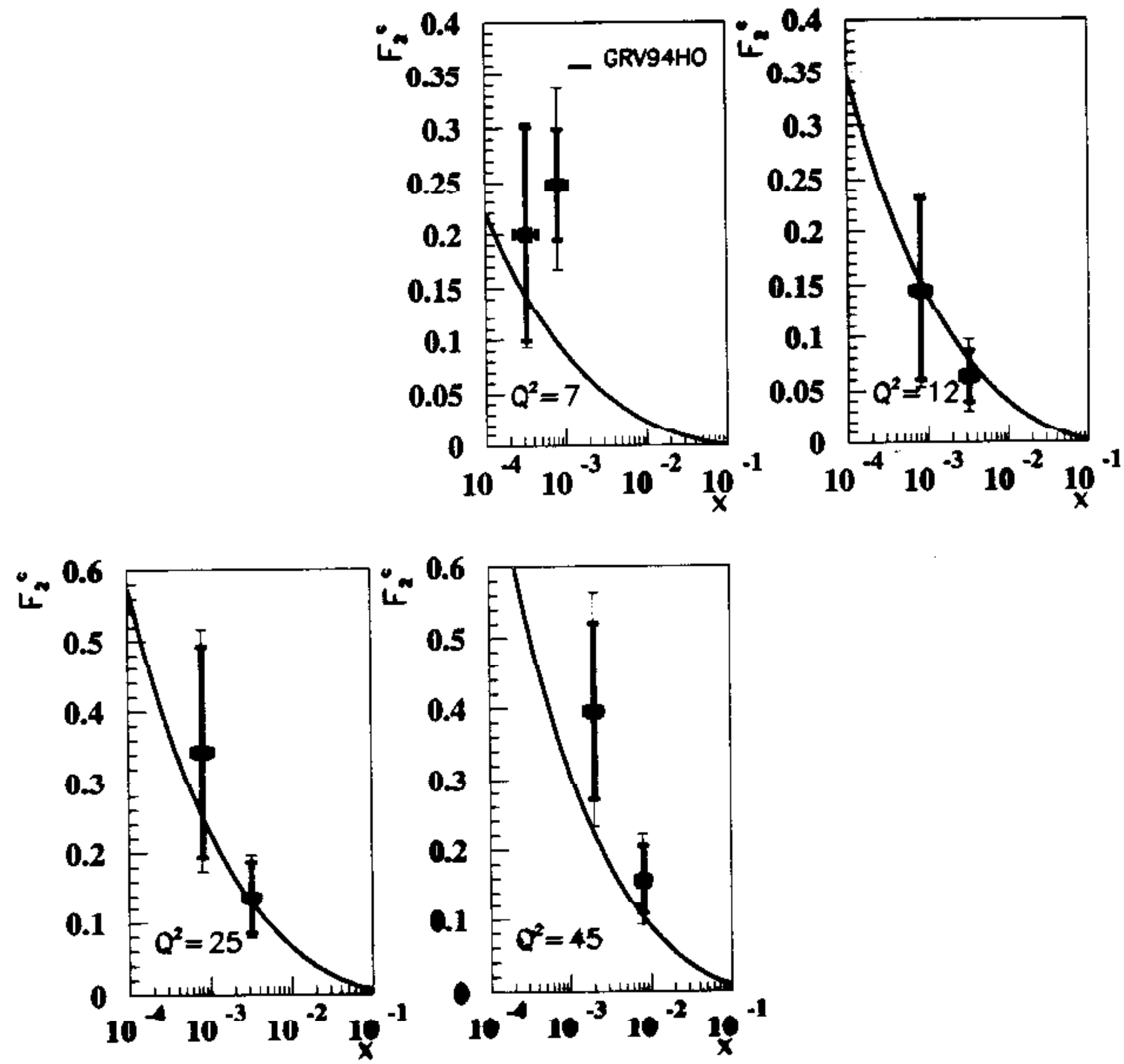

H1 94

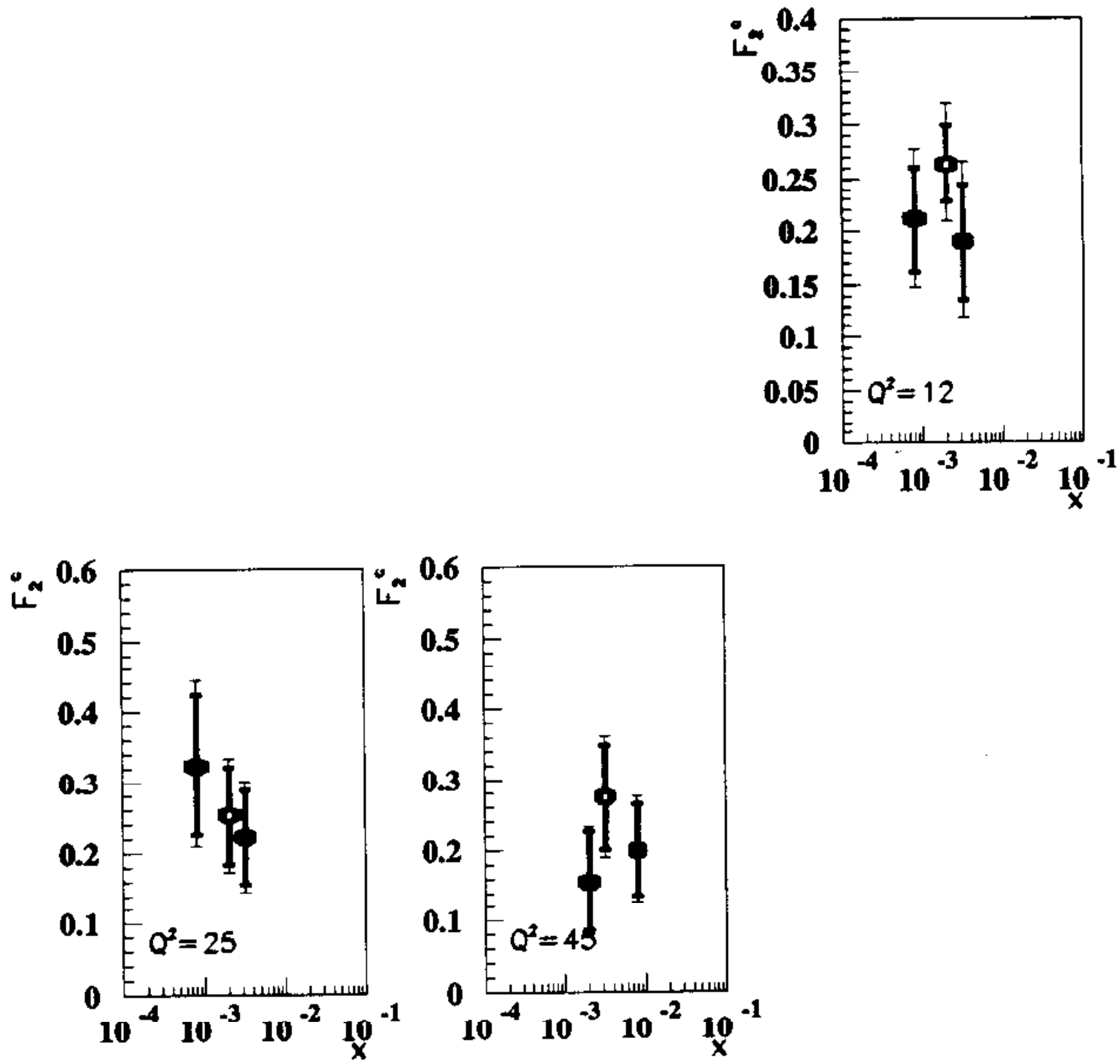
F_2^c
0.4
0.35
0.3
0.25
0.2
0.15
0.1
0.05
0
Q^2= 12
10^{-4} 10^{-3} 10^{-2} 10^{-1}
x
F_2^c
0.6
0.5
0.4
0.3
0.2
0.1
0
Q^2= 25
10^{-4} 10^{-3} 10^{-2} 10^{-1}
x
F_2^c
0.6
0.5
0.4
0.3
0.2
0.1
0
Q^2= 45
10^{-4} 10^{-3} 10^{-2} 10^{-1}
x

Summary

- **D**$^{*\pm}$ total and differential cross sections are measured in a restricted kinematic region → direct measurement

- NLO PGF pQCD calculations give good description of DATA but predictions lie a bit below measurements

- PGF prediction describes well DATA (x_{D^*} distribution)

- $\sigma_{c\bar{c}}$ cross sections estimated by extrapolation to the full p_T,η range of D* → not a direct measurement

- $F_2^{c\bar{c}}$ is found to rise rapidily as x decreases. The rise is described by NLO QCD calculations when using a gluon density consistent with that extracted from the scaling violations in the proton structure function F_2 measured at HERA.
- $F_2^{c\bar{c}}$ measurement gives in independent check of the gluon density.

- the ratio $F_2^{c\bar{c}}/F_2$ is about 25% for the entire range of (Q^2,x) of the present study

- GRV94, CTEQ4F3 give same predictions and close to the "MRRS."